

INVESTIGATIONS ON SOLAR THERMAL PROCESS HEAT INTEGRATION WITH PARABOLIC TROUGH COLLECTORS

Heinz Marty and Elimar Frank

HSR University of Applied Science of Rapperswil,
Institut fuer Solartechnik SPF, 8640 Rapperswil (Switzerland)

1. Abstract

The integration of solar heat in industrial processes has a huge potential, but up to now most of the solar thermal plants that are operated for the heat delivery to industrial processes are small scale pilot plants. First and simple assessments of the integration options and the expected solar energy yields may often lead to a basic feasibility decision. If parabolic trough collectors are used, the orientation of the rows is one of the planning parameters to be decided. Based on the early planning phase of a SHIP plant in Switzerland, the calculations presented in this paper may serve as a first indicator for planning decisions regarding the orientation of parabolic trough collector fields for latitudes in central Europe. For the configuration of a parabolic trough collector field, not only the yearly specific or total energy yields but also the course of direct irradiance and peak power over a day and the distribution over months can help to optimize the cost-benefit ratio of the solar heat plant. However, depending on technical, economical or other boundary conditions (marketing, vacation close-down of the company etc), a solar heat plant concept which is not leading to the highest specific yields may be chosen.

2. Introduction

In recent years, the huge potential of the integration of solar heat into industrial processes has been addressed (cf. <http://www.iea-shc.org/task33/publications/index.html>). Potential studies for a number of European countries have been carried out, showing that e.g. the solar heat integration for industrial processes (SHIP) in Austria is in the range of 3 GW_{th} and 100..125 GW_{th} are estimated to be the solar process heat contribution potential for the EU-25 countries (cf. Vannoni et al., 2008). Nevertheless, SHIP is still at an early stage of development. Many of the solar thermal plants that are operated for the heat delivery to industrial processes are small scale pilot plants. In Switzerland, several demonstration plants have been built since 2010 or are currently in the planning phase (cf. SFOE, 2011). In this paper, one of those plants in the planning phase is taken as a starting point to focus on the solar thermal process heat integration using parabolic trough collectors at that site and more general at similar latitudes. The company is located nearby Fribourg in Switzerland and produces dairy products. A gas driven boiler delivers process steam to a network at 175 °C and 9 bar.

3. Solar heat integration options

Basically, three general options can be considered:

- Integration option #1: In parallel to the existing steam boiler (labelled with #1 in Fig 1) a second solar heat driven steam boiler could be installed also feeding steam to the net at 9 bar and 175°C (or above).
- Integration option #2.1 and #2.2: Heating-up of the steam boiler feed water (between 10 and 8 in Fig 1 or between 8 and 9). At the site, the heat demand at these integration points by far exceeds the yield of a solar field of less than 1000 m² gross area.
- Integration option #3: Direct solar heat delivery to one or more specific thermal process(es), represented, for example, with label #3in Fig 1.

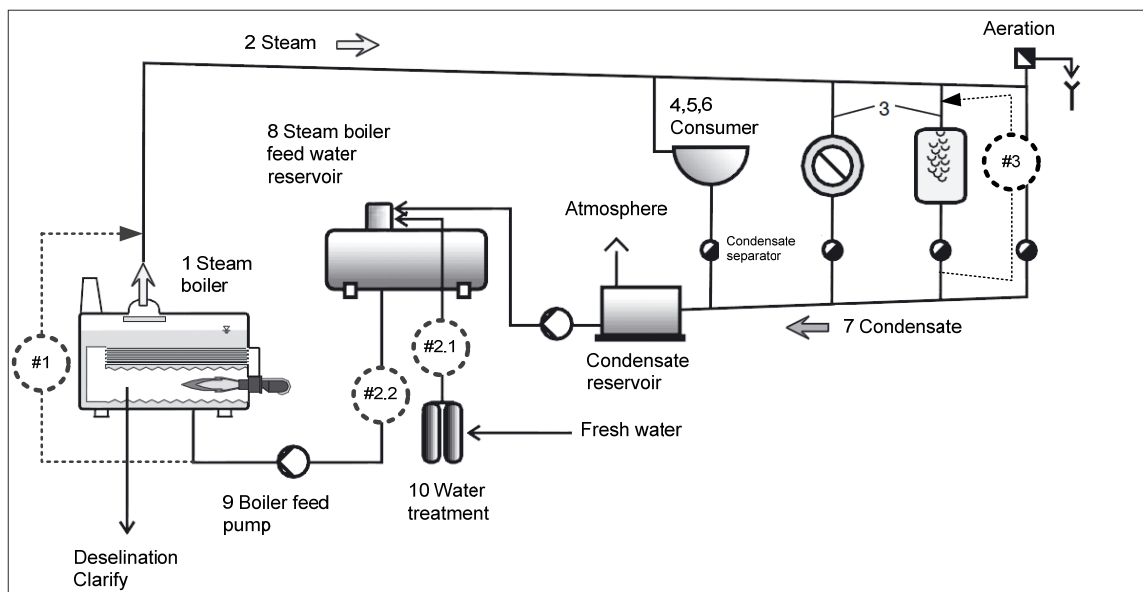


Fig 1: Illustration of a process steam network with open condensate reservoir and several options to integrate solar heat, source: www.spiraxsarco.com, adapted by the authors.

The company decided that their preferential aim is to have a very high solar fraction of heat for one specific pasteurization process due to the configuration of the production site, marketing reason and minimal modifications on the heat distribution system. The process considered in this case study must be fed by steam at 6 bar and 165 °C. The process is operating 5 days per week and continuously about 10 h per day. The time of the process start can be freely chosen. It is possible to schedule the process in a way so that the process halftime is reached at solar noon. The process steam demand while the process is active (at 165°C and 6 bar) accounts to approximately 300 kW and can be considered as constant. Thus, to reach a maximum solar heat integration without an additional storage or heat sink for the solar heat during the operation time of the process, the collector aperture area of the solar plant would roughly be in the range of 550..670 m² (assuming a maximum/minimum collector efficiency of 0.55 and 0.45, respectively, and taking no other effects into account). The roof available has a size of about 40m by 20m with an inclination of 16° facing south. On those two days when the specific process is not active, the energy supply of the solar plant can be delivered to the local heat network that is operated with a return temperature of 80°C. The energy supply of the heat network which feeds several processes is around 8'700kWh/a, so that also for the tow days when the specific process is not active any deactivation of the solar plant could be avoided without an additional storage for solar heat. Nevertheless, delivering solar heat to the heat network should only be done if there is excess heat because the heat from the local network is supplied externally with less than 40 US\$/MWh (exchange rate of August, 2011).

4. Assessment of the solar energy yield for north-south and east west orientation

Focusing on integration option #3, in this section the solar energy yield for a parabolic trough collector field is assessed with orientations north-south (NS) and east-west (EW). Several steps have been carried out:

- Calculations of the direct irradiance and irradiation on a one-axis tracked surface
- Calculation of the end effect correction and the Incidence Angle Modifier (IAM) for specific parabolic trough collector configurations
- Calculation of the yearly solar energy yields taking into account the collector efficiency

Direct irradiance and irradiation on a one-axis tracked surface

In a first step, the direct irradiance on a one-axis tracked surface is calculated for two orientations (NS and EW). Several generalizations have been made: The roof is assumed to be horizontal and not shaded, and the one-axis tracking is ideal. The roof dimensions are 40m east-west and 20m north-south.

For the calculation of the direct irradiance, climate data from Meteotest (www.meteotest.ch) have been used. They are based on longtime measured values for weather stations nearby (Payerne: Global irradiation 1159kWh/m².a, DNI, 1041kWh/m².a; Plaffeien: Global irradiation 1171kWh/m².a, DNI, 1150kWh/m².a) and extrapolated for the location of Fribourg in Switzerland (Swiss midlands, latitude 47°N, longitude 7°E, 588m above sea level) with the software Meteonorm by Meteotest. For the calculation of the direct irradiance on one-axis tracked surfaces, a routine has been programmed and integrated in the software Polysun¹ and simulations have been carried out with one-hour time steps.

Thus, the direct irradiance (DI) on an imaginary one-axis tracked surface with no inclination and an ideal tracking accuracy describes which fraction of the total irradiance is basically usable for a one-axis tracked concentrating solar collector. In Fig 2, a typical daily course for the DI for a summer day without clouds at the location of Fribourg is shown. The NS-oriented surface has peaks in the morning and evening because then the cosine factor for the conversion of the irradiance onto a tilted surface equals one. An EW-oriented surface has only one peak during a day without clouds that occurs when the solar azimuth angle is zero because only then the cosine factor equals one. The peak of the EW-oriented surface (959 W/m², hourly mean value) is only slightly higher (about 5%, relative) than for the NS-orientation. However, the total direct irradiation on that specific day is much lower for EW (8.65 kWh/m²d) than for NS (11.88 kWh/m²d). In winter, the courses of DI are similar (cf. Fig 3) with a reduced time frame for both orientations due to different times of sunrise and sunset. In winter, the direct irradiance on the EW-oriented surface is significantly higher (reaching about 200% of the maximum of the NS-orientation) and the peak of EW still reaches high values (789W/m², hourly mean value). In contrary to the day in summer, the daily direct irradiation in winter is much higher for EW (4.16 kWh/m²d) than for NS (2.32 kWh/m²d).

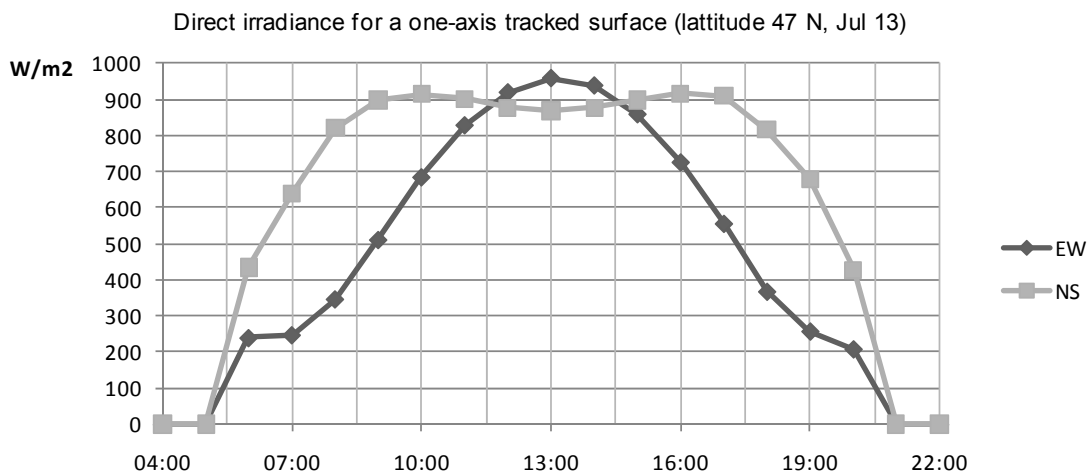


Fig 2: Daily course of the specific direct irradiance onto an imaginary one-axis tracked surface on a summer day without clouds for the location of Fribourg/Switzerland (Swiss midlands, latitude 47°N, longitude 7°E, 588m above sea level). The direct irradiance is calculated with Polysun and based on Meteonorm weather data.

¹ Polysun Version 5.7.11 15184, cf. www.velasolaris.com.

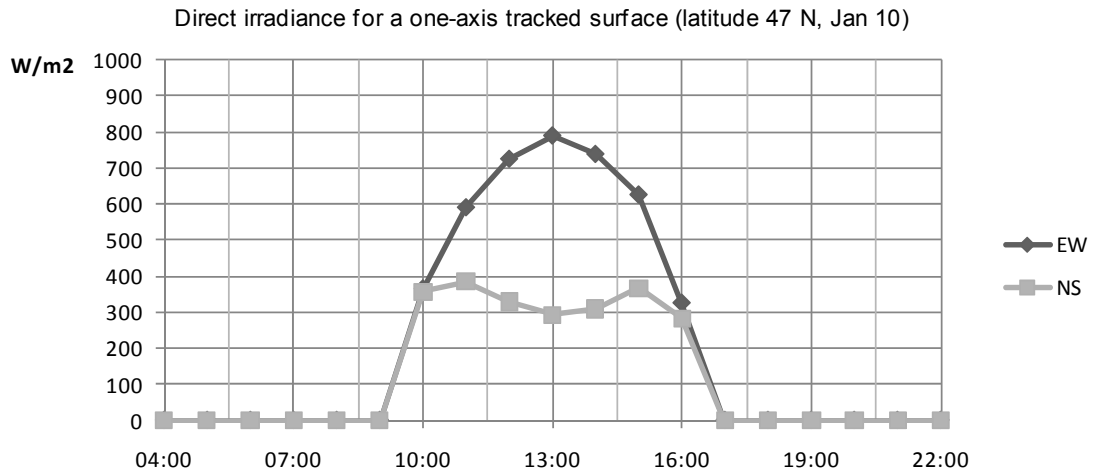


Fig 3: Daily course of the specific direct irradiance onto an imaginary one-axis tracked surface on a clear winter day for the location of Fribourg/Switzerland (Swiss midlands, latitude 47°N, longitude 7°E, 588m above sea level). The direct irradiance is calculated with Polysun and based on Meteonorm weather data.

In Fig 4, the monthly maxima of the direct irradiance on one-axis tracked surfaces for both NS and EW orientation are shown. The peak levels of the EW oriented surface are higher (or approx. the same for June, July and August) than those of the NS field and show less variation over the year. In terms of monthly direct irradiation, Fig 5 shows that NS has higher values in summer and lower values in winter (up to about +/- 40%, relatively) for this latitude, just as Fig 2 and Fig 3 indicate. With higher latitudes, the differences increase. For the whole year, the total direct irradiation sums up to 804 kWh/m²a in case of EW and 959 kWh/m²a, which is a plus of 16% (relatively).

Summarizing, EW reaches higher values for direct irradiance both in summer and winter and also higher daily and monthly irradiation in winter, but the yearly direct irradiation is significantly higher for NS. However, the maxima of monthly direct irradiance and the monthly direct irradiation are varying less for EW.

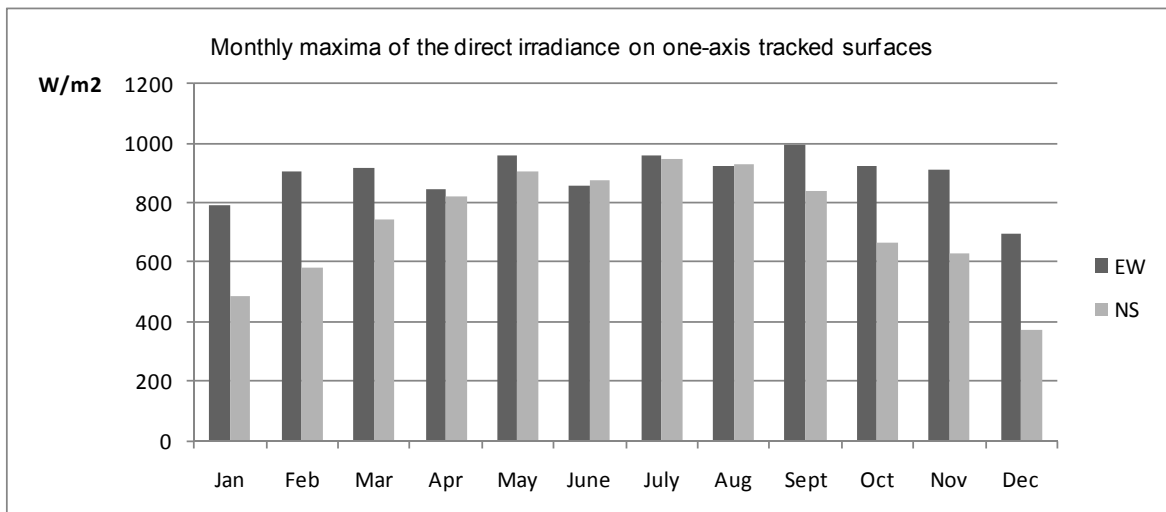


Fig 4: Monthly maxima of the direct irradiance on one-axis tracked surfaces for EW and NS orientation for the location of Fribourg/Switzerland (Swiss midlands, latitude 47°N, longitude 7°E, 588m above sea level).

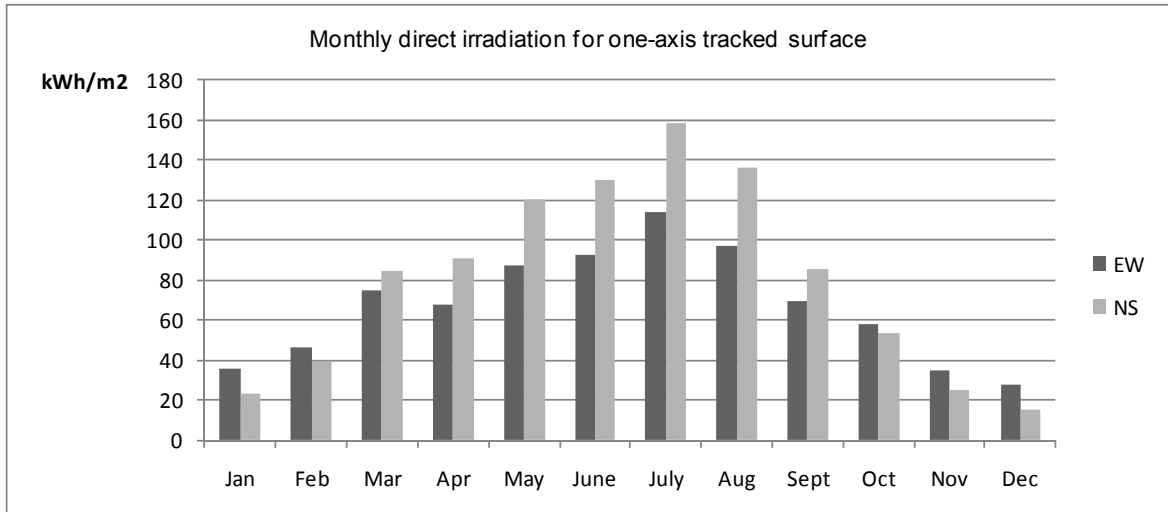


Fig 5: Monthly direct irradiation for one-axis tracked surfaces for EW and NS orientation for the location of Fribourg/Switzerland (Swiss midlands, latitude 47°N, longitude 7°E, 588m above sea level).

Calculation of the end effect correction and the Incidence Angle Modifier (IAM) for specific parabolic trough collector configurations

Following Duffie and Beckman (2006) the end effect correction κ can be calculated depending on the aperture width (a), the length of the trough (l), the focal length (f) (which is the distance from the focal point to the vertex) and the incidence angle θ :

$$\kappa = 1 - \frac{f}{l} \cdot \frac{a^2}{48 \cdot f^2} \cdot \tan(\theta) \quad \text{eq. (1)}$$

Appointing $f = 0.65\text{m}$ and $a = 1.2\text{m}$, the end effect correction is shown in Fig 6 for different trough lengths (5, 10, 20 and 40m).

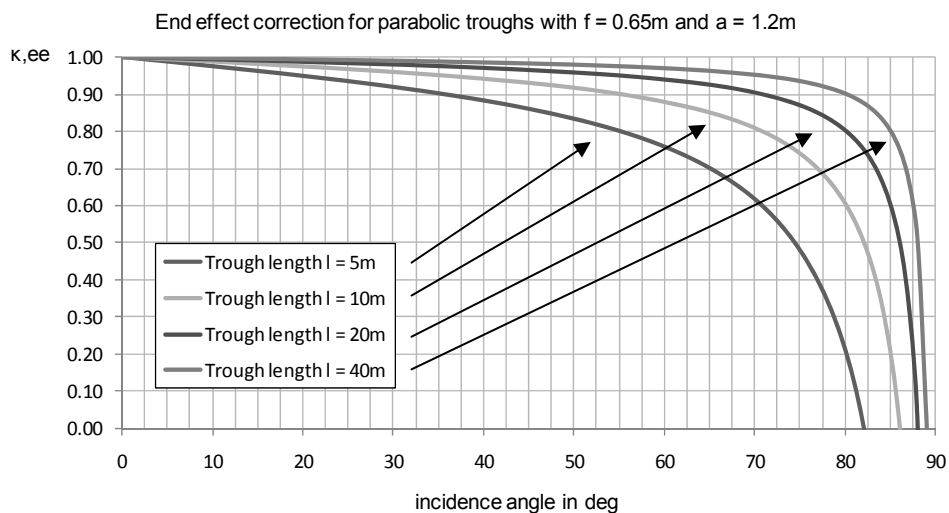


Fig 6: Calculation of the end effect correction for parabolic troughs based on eq. (1) for $f = 0.65\text{m}$ and $a = 1.2\text{m}$ and different trough lengths.

Furthermore, the collector model that is implemented in Polysun includes the option to define Incident Angle Modifiers (IAM) in one-degree resolution. Fig 7 shows the IAM longitudinal of the collector that has been used for further calculations.

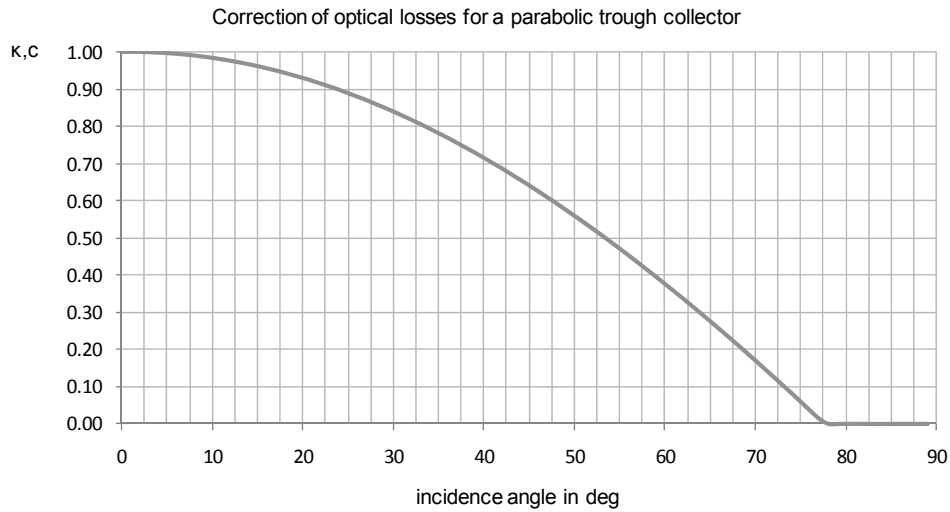


Fig 7: Specific Incident Angle Modifier (IAM) for a parabolic trough that has been used for the calculations in this paper.

Calculation of the yearly solar energy yields

Based on the assessment of the direct irradiation on one-axis tracked surfaces (as described above) a solar energy yield can be calculated choosing parabolic trough collectors to supply heat. For this, the end effect correction, the IAM and the collector efficiency have to be considered. For the efficiency curve, the following parameters have been used: $\eta_{a0} = 0.685$, $c_1 = 0.4 \text{ W/m}^2/\text{K}$, $c_2 = 0.0015 \text{ W/m}^2/\text{K}^2$. Dynamic effects like system control, heating-up of the thermal capacity (especially in the morning), shading effects of clouds (in minute time resolution) and effects/losses of the piping etc. are not addressed. For the calculations, the roof area is not shaded and horizontal with dimensions of 40m east-west and 20m north-south. Instead of the imaginary surfaces of the sections above, now two collector fields are defined: EW with trough lengths of 40m and a row spacing of 1.8m (=1.5*aperture) and NS with trough lengths of 20m and a row spacing of 2.4m (=2.0*aperture). Based on these assumptions, shading effects due to row spacing are similar for both orientations and can be neglected for the comparison. The EW configuration has an aperture area of 576 m² (72% of the gross roof area) and the NS configuration an aperture area of 408 m² (51% of the gross roof area). However, it has not been taken into account that the trough lengths depend on module lengths of the collectors and are not arbitrary which, together with the aperture and the row spacing, influences the gross roof area usage ratio. Furthermore, the yield has been assessed assuming that solar heat is always supplied by the parabolic trough collector field if the efficiency is greater than zero and assuming that the solar heat can always be fed into the process. For the integration, three different mean collector temperatures T_m have been set (165°C, 150°C, 135°C).

Fig 8 shows the monthly energy yields for the one-axis tracked parabolic trough collector fields as described before with EW and NS orientation for $T_m = 165^\circ\text{C}$. The specific monthly energy yield is presented on the left axis and the total monthly energy yield of the respective aperture areas on the right axis. The distribution of the specific energy yield is similar to Fig 5 but now including the end effect correction, the IAM and the collector efficiency. Naturally, all specific values are lower for the yield than for the direct irradiances, and mainly due to the different IAM factors, the differences between EW and NS regarding the specific energy yields are higher than the differences of the direct irradiation on one-axis tracked surfaces.

Although the aperture area of the EW orientated field is 41% larger than of the NS-orientated field, in summer the specific energy yields as well as the total energy yields are significantly higher for NS. The

yearly total energy yield in case of EW sums up to 136 MWh/a which is even less (almost 4%) than the yearly total energy yield of the NS orientated field (141 MWh/a). This is also confirmed by the **yearly** specific energy yield which is significantly smaller for EW (236 kWh/m²a) than for NS (345 kWh/m²a).

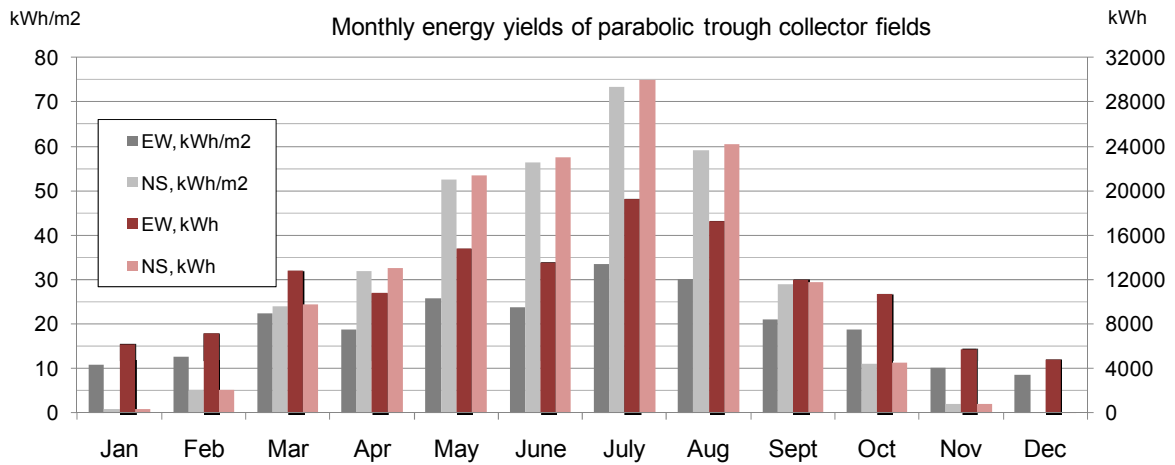


Fig 8: Monthly energy yields of an EW-orientated (576m² aperture area, row length 40m, row spacing 1.5*aperture) and a NS-orientated (408m² aperture area, row length 20m, row spacing 2.0*aperture) parabolic trough collector field. On the left axis, the monthly specific energy yields for both orientations are displayed, on the right axis the monthly total energy yield. The results have been calculated using hourly values for the direct irradiance on one-axis tracked surfaces, the IAM factors and the collector efficiency for $T_m = 165^\circ\text{C}$ at the location of Fribourg/Switzerland (Swiss midlands, latitude 47°N , longitude 7°E , 588m above sea level).

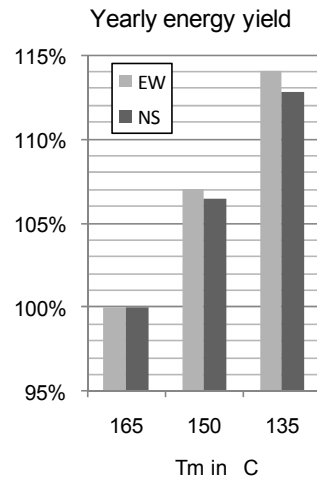


Fig 9: Yearly energy yields of both EW and NS orientated fields for different mean collector temperatures T_m , normalized to the yields achieved with $T_m = 165^\circ\text{C}$

While Fig 8 is showing energy yields assuming a collector mean temperature of 165°C , the mean collector temperature may vary depending on the control, the flow rates in the collector circuit, the heat exchanger area for the integration of the solar heat, the process temperature etc. Fig 9 shows the yearly total energy yields of both EW and NS orientated fields, normalized to the yields achieved with $T_m = 165^\circ\text{C}$. The monthly distribution is qualitatively the same as what has been shown for $T_m = 165^\circ\text{C}$ in Fig 8, and the relative deviation of the specific yearly yield is the same as for the total yearly yield. Lowering T_m to 150°C would increase the solar energy yield by about 7.0% (EW) or 6.4% (NS), and lowering T_m to 135°C would increase the solar energy yield by about 14.0% (EW) or 12.8% (NS).

5. Summary and conclusions

For the integration of solar heat in industrial processes, several integration options and connected with that also several technological options for the collector have to be compared. In the early planning phase of a SHIP plant for a company in Fribourg/Switzerland, the question came up whether a north-south orientation or an east-west orientation of a parabolic trough collector field is favourable. Amongst other influences, the latitude of the location (47°N in this case) plays a central role.

In a first step, the specific direct irradiance and irradiation for one-axis tracked surfaces has been analyzed. EW reaches higher values for direct irradiance both in summer and winter and also higher daily and monthly irradiation in winter, but the yearly direct irradiation is significantly higher for NS. However, the maxima of monthly direct irradiance and the monthly direct irradiation are varying less for EW.

For calculating the solar energy yields of parabolic trough collector fields, an end effect correction was calculated for chosen collector geometry parameters, and an IAM as well as a collector efficiency curve has been set. Taking a horizontal roof with 40m east-west and 20m north-south, the maximum aperture areas for EW (576m²) and NS (408m²) have been assessed assuming an aperture width of 1.2m, row lengths of 40m (EW) or 20m (NS) and row spacing of 1.5*aperture (EW) and 2.0*aperture (NS) so that row shading does not make a difference for the yield comparison of the fields.

With some simplifications (e.g. assuming that solar heat can always be used if provided at a temperature high enough), the monthly and yearly energy yields for the one-axis tracked parabolic trough collector fields with EW and NS orientation have been analyzed for $T_m = 165^\circ\text{C}$. The energy supply of EW is distributed more evenly over the year, however, although the aperture area of the EW orientated field is 41% higher than of the NS-orientated field, the yearly total energy yield in case of EW sums up to 136 MWh/a which is even less (almost 4%) than the yearly total energy yield of the NS orientated field (141 MWh/a). Also, the yearly specific energy yield is significantly smaller for EW (236 kWh/m²a) than for NS (345 kWh/m²a). However, if the process heat demand profile limits the solar energy supply, e.g. the specific energy yield for NS which was higher than for EW is decreasing because NS has significantly longer daily operation times in summer. In that case, either a storage or a different field orientation could be advantageous

If the yields are calculated with lower mean collector temperatures, a relative increase of the solar energy yield compared with $T_m = 165^\circ\text{C}$ by about 7.0% (EW) or 6.4% (NS) for $T_m = 150^\circ\text{C}$ and 14.0% (EW) or 12.8% (NS) for $T_m = 135^\circ\text{C}$ can be expected.

The calculations presented in this paper may serve as a first indicator for planning decisions regarding the orientation of parabolic trough collector fields for latitudes in central Europe. For the configuration of a parabolic trough collector field, not only the yearly specific or total energy yields but also the course of direct irradiance and peak power over a day and the distribution over months can help to optimize the cost-benefit ratio of the solar heat plant. However, depending on technical, economical or other boundary conditions (marketing, vacation close-down of the company etc), a solar heat plant concept which is not leading to the highest specific yields may be chosen. Yet, the true energy yield can only be calculated simulating the process heat demand, piping losses, dynamic collector and collector field effects etc.

References

- Duffie, J, Beckman, W., 2006: Solar Engineering of Thermal Processes, 3rd Edition, Wiley, Canada.
- SFOE, 2011: Swiss Federal Office of Energy, Industrial Use of Solar Energy Research Programme: Project reports, <http://www.bfe.admin.ch/forschungindustriesolar/>
- Vannoni, C., Battisti, R., Drigo, S., 2008: Potential for Solar Heat in Industrial Processes. Report of IEA-SHC Task 33, Solar Heating and Cooling Executive Committee of the International Energy Agency.